Electronic Supplementary Material (ESI) for Journal of Materials Chemistry A.

Electronic Supplementary Material (ESI)

Theoretical Investigation of Zirconium Carbide Mxenes as Prospective High Capacity Anode Materials for Na-ion Batteries

Qiangqiang Meng,[a,b] Jiale Ma,[a] Yonghui Zhang,[a] Zhen Li,[a] Alice Hu,[c] Ji-Jung Kai [c], and Jun Fan*[a,d]

[a] Department of Materials Science& Engineering, City University of Hong Kong, Hong Kong, China Email: junfan@cityu.edu.hk.

[b] Key Laboratory for Advanced Technology in Environmental Protection of Jiangsu Province, Yancheng Institute of Technology, Yancheng, Jiangsu 224051, China.

[c] Department of Mechanical and Biomedical Engineering, City University of Hong Kong, Hong Kong, China

[d] City University of Hong Kong Shenzhen Research Institute, Shenzhen 518057, China

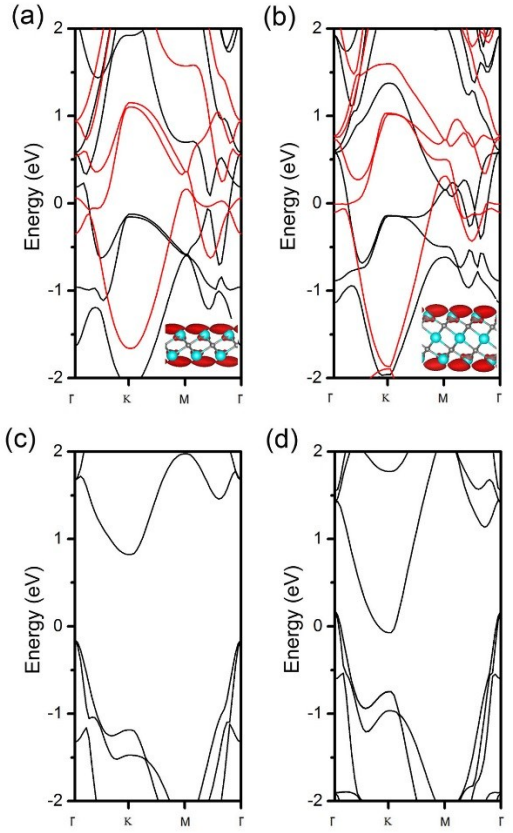

Figure S1 The band structures of the monolayer (a) Zr_2C (the inset is spin density of Zr_2C), (b) Zr_3C_2 (the inset is spin density of Zr_3C_2), (c) Zr_2CO_2, and (d) $Zr_3C_2O_2$, respectively. The Fermi level is set to zero.

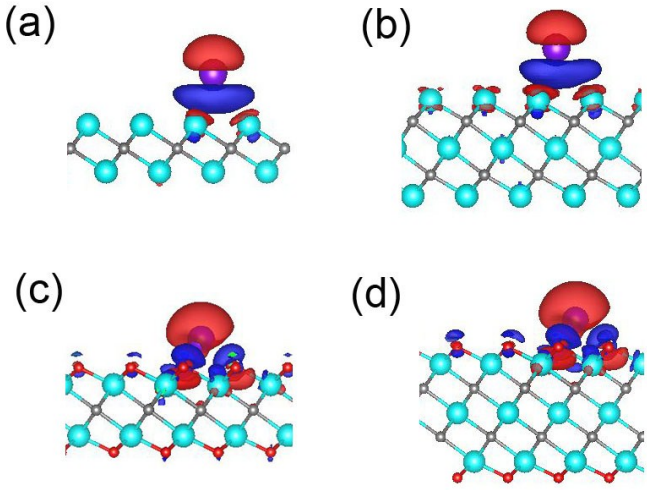

Figure S2 Charge density difference isosurfaces of single Na adsorbed on (a) Zr_2C, (b) Zr_3C_2, (c) Zr_2CO_2, and (d) $Zr_3C_2O_2$ monolayers. Isosurface level set to 0.007 e $Å^{-3}$. electron-rich regions, red; and electron-deficient regions, blue.

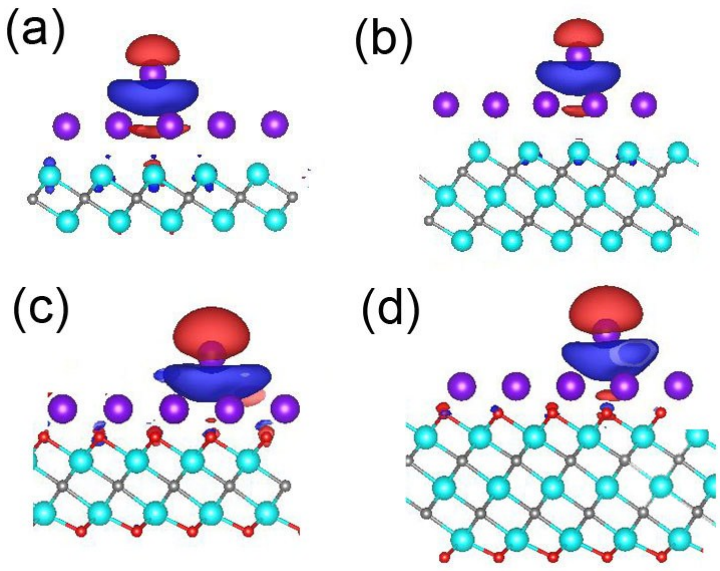

Figure S3 Charge density difference isosurfaces of single Na adsorbed on (a) Zr_2CNa_2, (b) $Zr_3C_2Na_2$, (c) $Zr_2CO_2Na_2$, and (d) $Zr_3C2O_2Na_2$ monolayers. Isosurface level set to 0.0035 e $Å^{-3}$. electron-rich regions, red; and electron-deficient regions, blue.

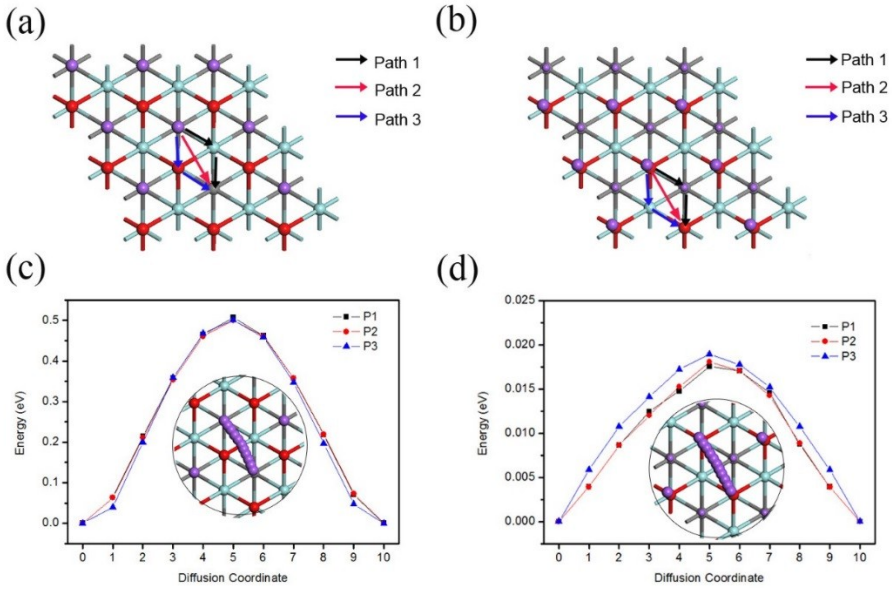

Figure S4 Considered migration paths of Na diffusion on the Zr_2CO_2 with high Na coverage, meanwhile P1, P2, and P3 represent possible migration paths for Na atoms for (a) first and (b) second layer Na atoms, respectively; the migration paths and corresponding diffusion energy barrier profiles for (c) first and (d) second layer Na atoms, respectively.

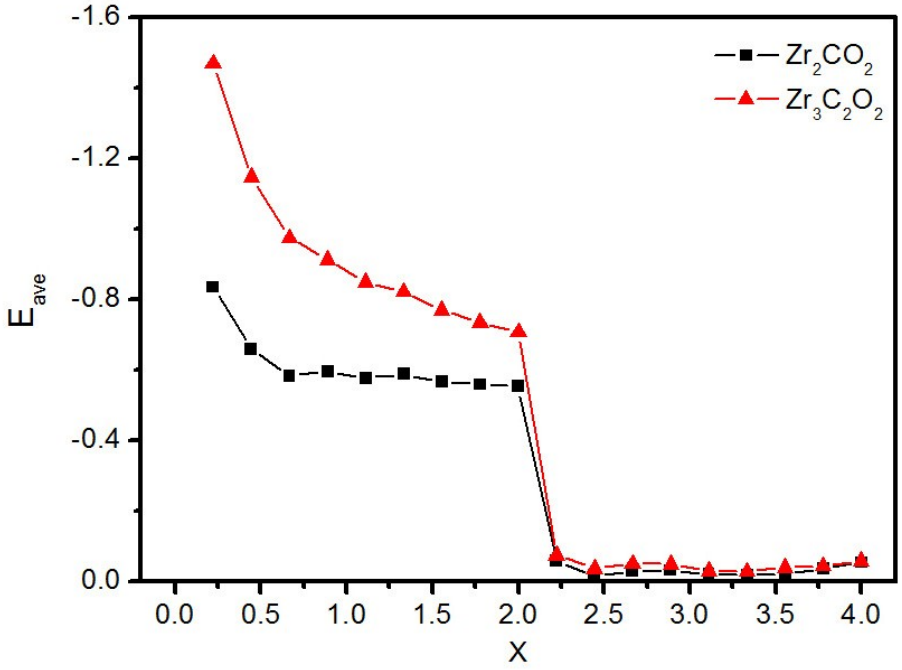

Figure S5 The E_{ave} as a function of x in $Zr_2CO_2Na_x$ and $Zr_3C_2O_2Na_x$.

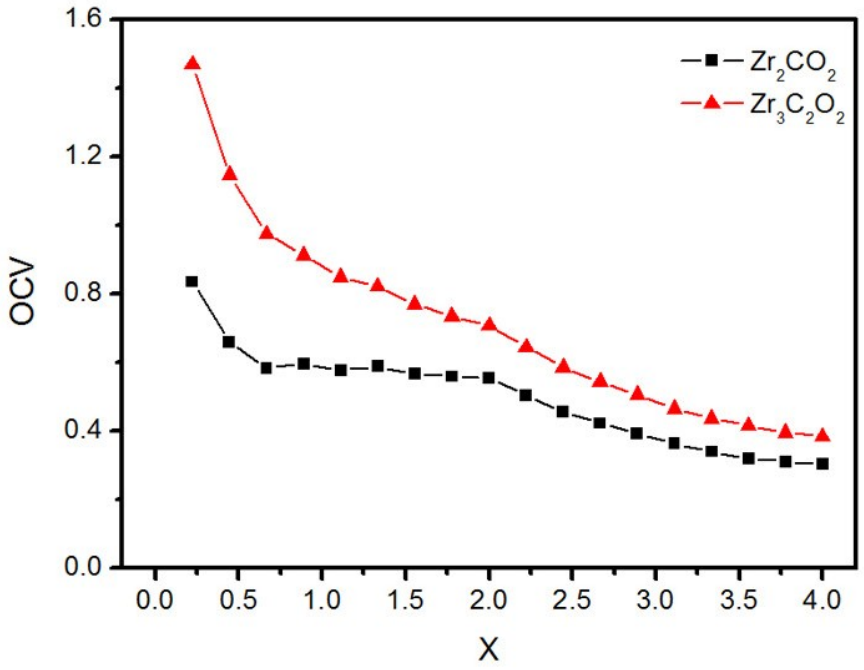

Figure S6 The OCV as a function of x in $Zr_2CO_2Na_x$ and $Zr_3C_2O_2Na_x$.

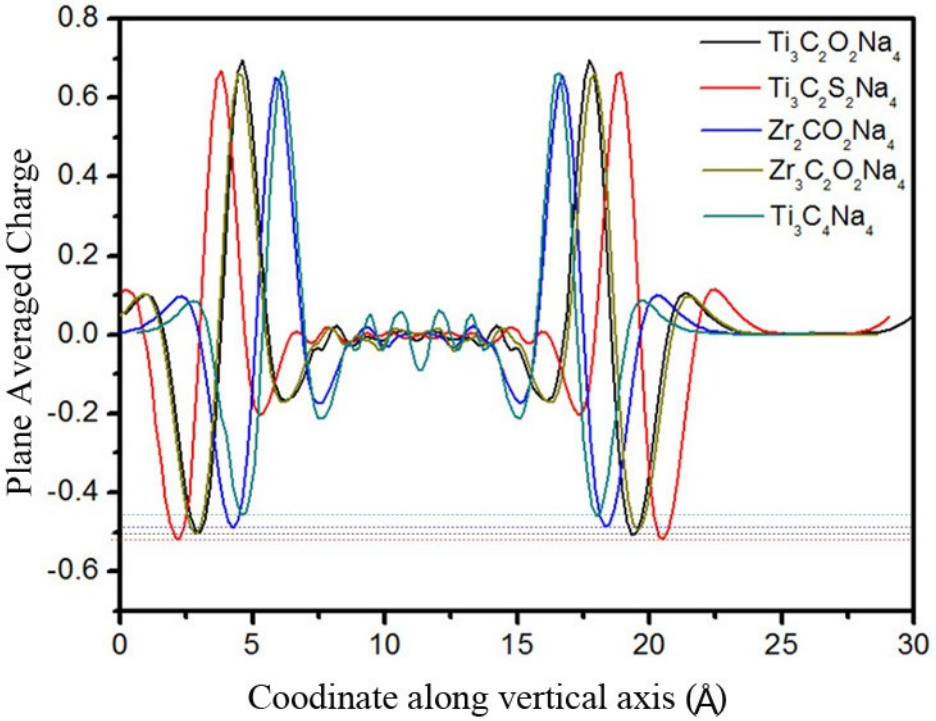

Figure S7 The difference in charge transfer of plane averaged charge for $Ti_3C_2O_2Na_4$, $Ti_3C_2S_2Na_4$, $Zr_2CO_2Na_4$, $Zr_3C_2O_2Na_4$ and Ti_3CNa_4 system, respectively.

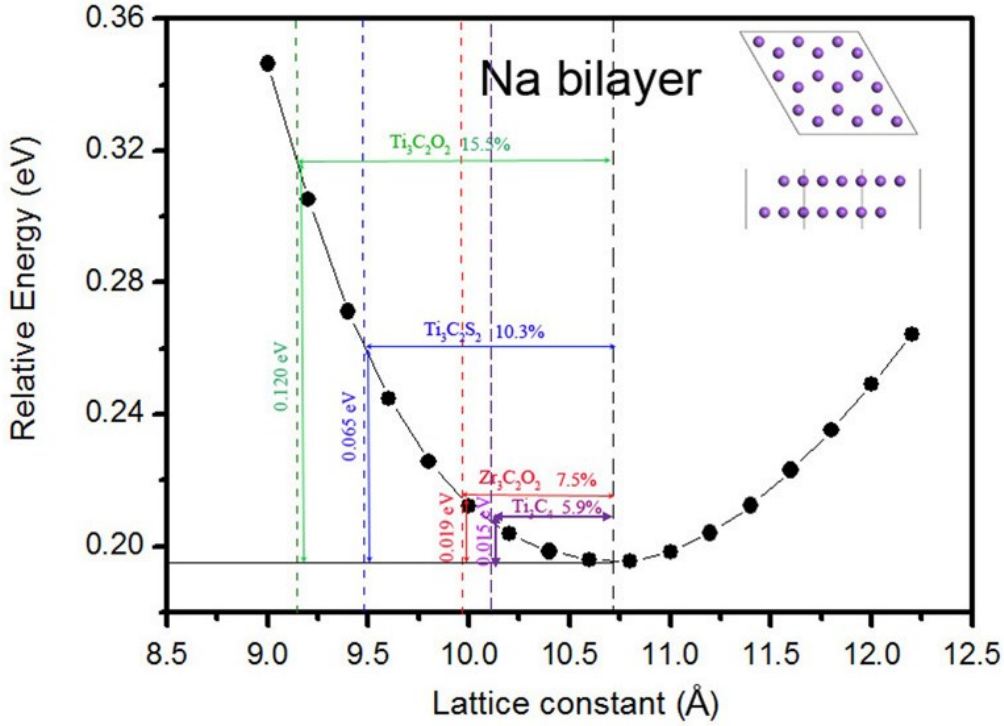

Figure S8 The relative energy as a function of lattice constant for Na bilayer with 3 × 3 super-cell (the schematic representations are shown in the insets), and the dash lines represent the lattice constants of $Ti_3C_2O_2$ (9.15 Å), $Ti_3C_2S_2$ (9.45 Å), $Zr_3C_2O_2$ (9.93 Å), Ti_3C_4 (10.11 Å) and Na bilayer (10.71 Å), respectively.

Table S1. Structure, magnetic moment and band gap of Zr_2C, Zr_3C_2, Zr_2CO_2 and $Zr_3C_2O_2$.

	Zr_2C	Zr_3C_2	Zr_2CO_2	$Zr_3C_2O_2$
Hexagonal lattice constant (Å)	3.32	3.34	3.31	3.31
Magnetic moment (μB)	1.90	1.73	nonmagnetic	nonmagnetic
Band gap (eV)	Metal	Metal	0.92	Metal

Table S2. Lattice constant (Å), Lattice mismatch, E_{ave} of the second layer Na atoms and Charge transfer value of $Ti_3C_2O_2$, $Ti_3C_2S_2$, Zr_2CO_2, $Zr_3C_2O_2$ and Ti_3C_4.

	$Ti_3C_2O_2$	$Ti_3C_2S_2$	Zr_2CO_2	$Zr_3C_2O_2$	Ti_3C_4
Lattice constant (Å)	3.05	3.15	3.31	3.31	3.37
Lattice mismatch [a]	15.5%	10.3%	7.5%	7.5%	5.9%
E_{ave} [b]	0.033	-0.01	-0.054	-0.059	-0.03
Charge transfer value [c]	-0.51	-0.52	-0.49	-0.51	-0.46

[a] Lattice mismatch is calculated compared with lattice constant of Na bilayer; [b] E_{ave} of the full second layer Na atoms; [c] charge transfer value of the second layer Na atoms is calculated from Figure S7.